
Sensorless Field Oriented Control (FOC) for a Permanent Magnet Synchronous Motor (PMSM) Using a PLL Estimator and Field Weakening (FW)

<i>Author: Mihai Cheles Microchip Technology Inc.</i>

INTRODUCTION

Current industry trends suggest the Permanent Magnet Synchronous Motor (PMSM) as the first preference for motor control application designers. Its strengths, such as high power density, fast dynamic response and high efficiency in comparison with other motors in its category, coupled with decreased manufacturing costs and improved magnetic properties, make the PMSM a good recommendation for large-scale product implementation.

Microchip Technology produces a wide range of Digital Signal Controllers (DSCs) for enabling efficient, robust and versatile control of all types of motors, along with reference designs of the necessary tool sets, resulting in a fast learning curve and a shortened development cycle for new products.

FIELD ORIENTED CONTROL (FOC)

In case of the PMSM, the rotor field speed must be equal to the stator (armature) field speed (i.e., synchronous). The loss of synchronization between the rotor and stator fields causes the motor to halt.

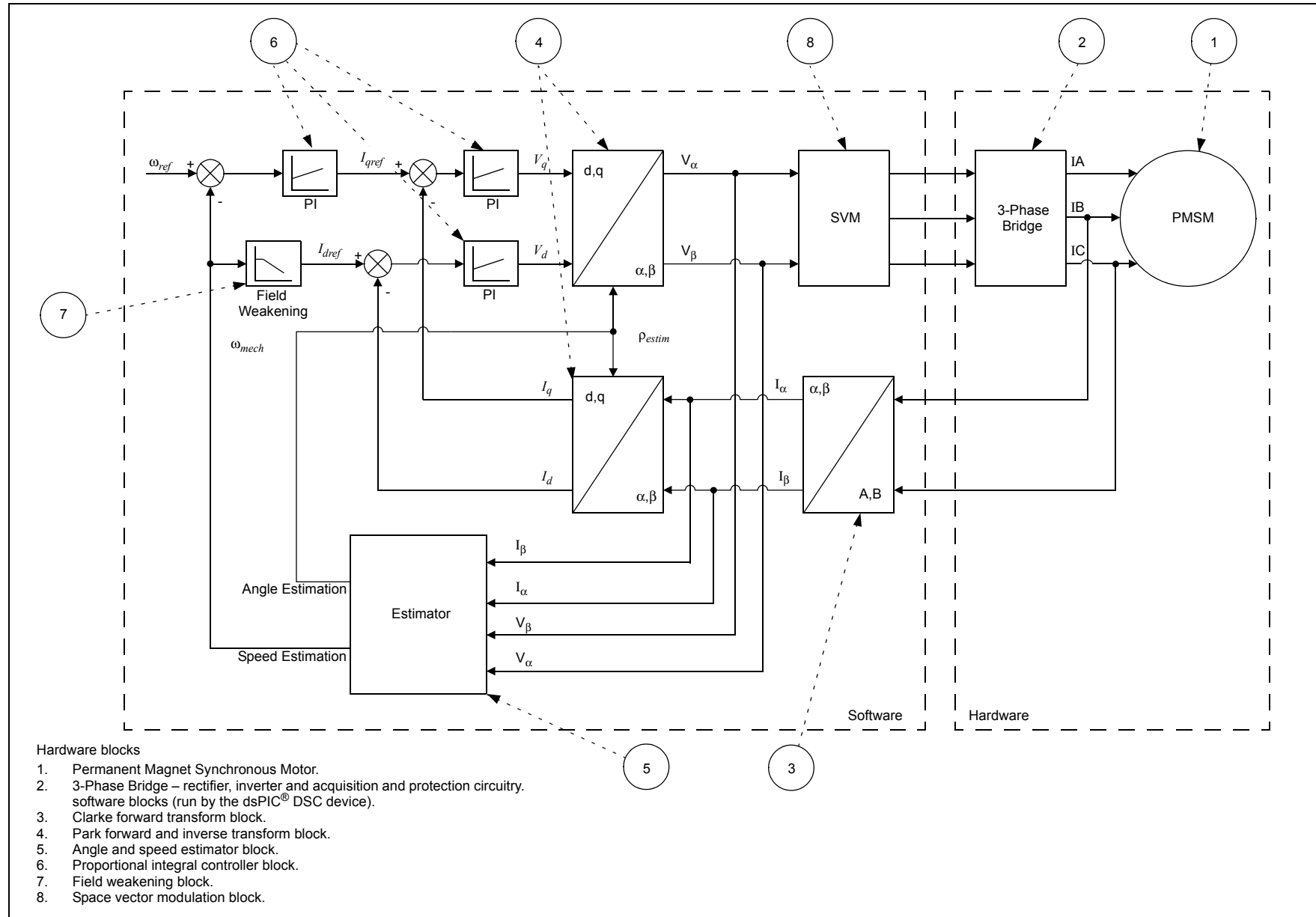
Field Oriented Control (FOC) represents the method by which one of the fluxes (rotor, stator or air gap) is considered as a basis for creating a reference frame for one of the other fluxes with the purpose of decoupling

the torque and flux-producing components of the stator current. The decoupling assures the ease of control for complex three-phase motors in the same manner as DC motors with separate excitation. This means the armature current is responsible for the torque generation, and the excitation current is responsible for the flux generation. In this application note, the rotor flux is considered as a reference frame for the stator and air gap flux.

Several application notes from Microchip explain the principles behind FOC. Two such examples are: AN1078 “*Sensorless Field Oriented Control of PMSM Motors using dsPIC30F or dsPIC33F Digital Signal Controllers*” and AN908 “*Using the dsPIC30F for Vector Control of an ACIM*” (see “**References**”). It is beyond the scope of this application note to explain the FOC details; however, the particulars of the new implementation will be covered with respect to the previously indicated application notes.

The control scheme for FOC is presented in Figure 1. This scheme was implemented and tested using the dsPICDEM™ MCLV Development Board (DM330021), which can drive a PMSM motor using different control techniques without requiring any additional hardware.

The control scheme is similar to the one presented in application note AN1162 “*Sensorless Field Oriented Control (FOC) of an AC Induction Motor (ACIM)*” (see “**References**”), except for the estimator particulars and obviously the motor used – a PMSM instead of an ACIM.

FIGURE 1: SENSORLESS FOC FOR PMSM BLOCK DIAGRAM


The particularity of the FOC in the case of PMSM is that the stator's d-axis current reference I_{dref} (corresponding to the armature reaction flux on d-axis) is set to zero. The rotor's magnets produce the rotor flux linkage, Ψ_{PM} , unlike ACIM, which needs a constant reference value, I_{dref} , for the magnetizing current, thereby producing the rotor flux linkage.

The air gap flux is equal to the sum of the rotor's flux linkage, which is generated by the permanent magnets plus the armature reaction flux linkage generated by the stator current. For the constant torque mode in FOC, the d-axis air gap flux is solely equal to Ψ_{PM} , and the d-axis armature reaction flux is zero.

On the contrary, in constant power operation, the flux generating component of the stator current, I_d , is used for air gap field weakening to achieve higher speed.

In sensorless control, where no position or speed sensors are needed, the challenge is to implement a robust speed estimator that is able to reject perturbations such as temperature, electromagnetic noise and so on. Sensorless control is usually required when applications are very cost sensitive, where moving parts are not allowed such as position sensors or when the motor is operated in an electrically hostile environment. However, requests for precision control, especially at low speeds, should not be considered a critical matter for the given application.

The position and speed estimation is based on the mathematical model of the motor. Therefore, the closer the model is to the real hardware, the better the estimator will perform. The PMSM mathematical modeling depends on its topology, differentiating mainly two types: surface-mounted and interior permanent magnet. Each type has its own advantages and disadvantages with respect to the application needs. The proposed control scheme has been developed around a surface-mounted permanent magnet synchronous motor (Figure 2), which has the advantage of low torque ripple and lower price in comparison with other types of PMSMs. The air gap flux for the motor type considered is smooth so that the stator's inductance value, $L_d = L_q$ (non salient PMSM), and the Back Electromagnetic Force (BEMF) is sinusoidal.

The fact that the air gap is large (it includes the surface mounted magnets, being placed between the stator teeth and the rotor core), implies a smaller inductance for this kind of PMSM with respect to the other types of motors with the same dimension and nominal power values. These motor characteristics enable some simplification of the mathematical model used in the speed and position estimator, while at the same time enabling the efficient use of FOC.

The FOC maximum torque per ampere is obtained by uninterruptedly keeping the motor's rotor flux linkage situated at 90 degrees behind the armature generated flux linkage (see Figure 3).

FIGURE 2: SURFACE MOUNTED PM PMSM TRANSVERSAL SECTION

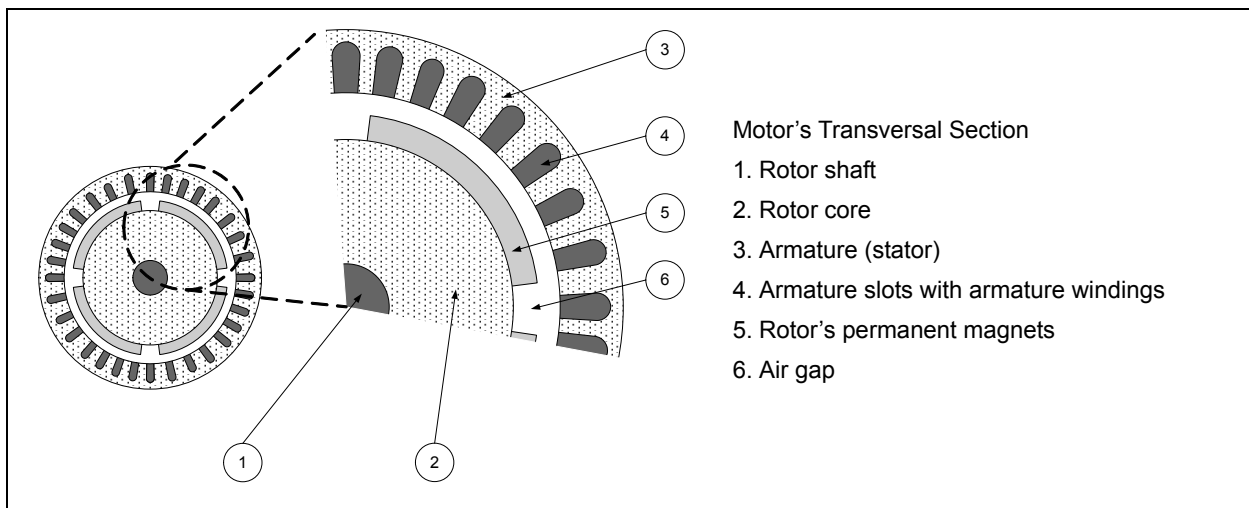
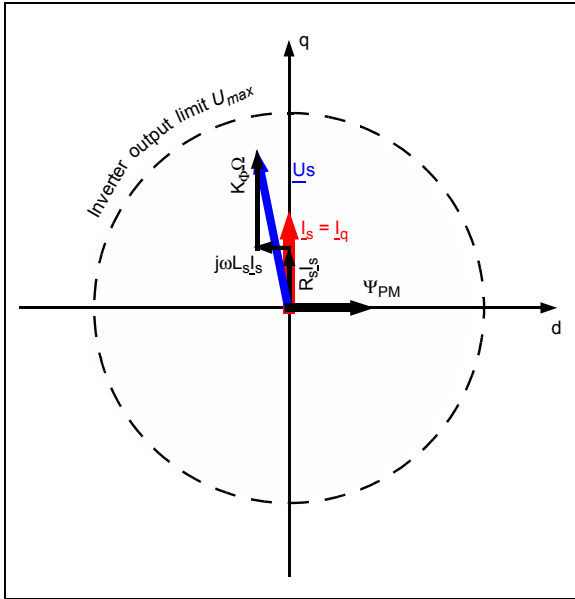
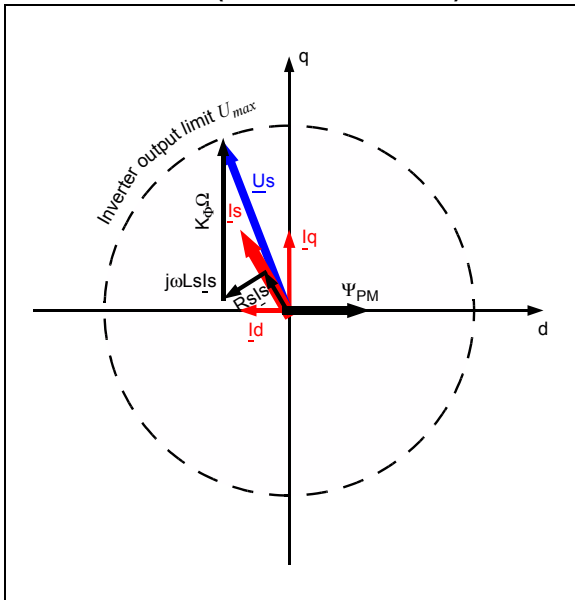


FIGURE 3: FOC PHASOR DIAGRAM (BASE SPEED)



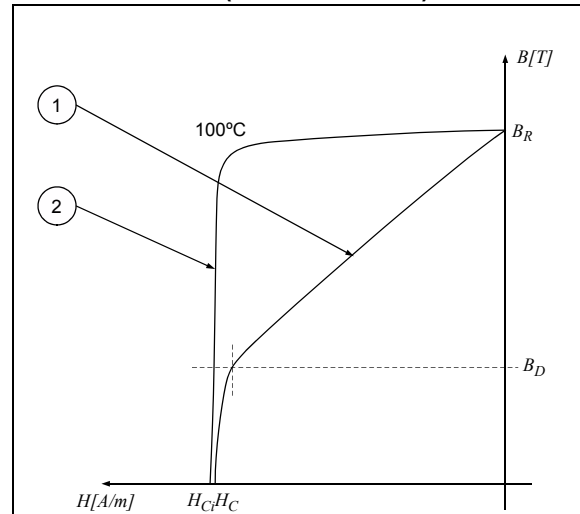
Considering the FOC constant power mode, the field weakening for the motor considered cannot be done effectively because of the large air gap space, which implies weak armature reaction flux disturbing the rotor's permanent magnets flux linkage. Due to this, the maximum speed achieved cannot be more than double the base speed for the motor considered for testing. Figure 4 depicts the phasors orientation in constant power – Field Weakening mode.

FIGURE 4: FOC PHASOR DIAGRAM (HIGH SPEED - FW)



CAUTION: During field weakening of a Surface Permanent Magnet (SPM) type of PMSM, mechanical damage of the rotor and the demagnetization of the permanent magnets is possible if careful measures are not taken or the motor manufacturer's specifications are not followed. The permanent magnets are usually bonded with an epoxy adhesive or affixed with stainless steel or carbon fiber rings. Beyond the maximum speed indicated by the manufacturer, the magnets could unbind or break, leading to destruction of the rotor, along with other mechanical parts attached to the motor's shaft. Demagnetization can be caused by exceeding the knee of flux density, B_D , for the air gap flux density, as indicated in Figure 5.

FIGURE 5: HYSTERESIS GRAPH OF PERMANENT MAGNET (THEORETICAL)



Hysteresis Graph

1. Intrinsic characteristic of permanent magnet.
2. Normal characteristic of permanent magnet.

Where:

H = Field intensity

B = Field induction

B_R = Permanent induction value

H_C = Coercivity

H_{Ci} = Intrinsic coercivity

PLL TYPE ESTIMATOR

The estimator used in this application note is an adaptation of the one presented in AN1162 “Sensorless Field Oriented Control (FOC) of an AC Induction Motor (ACIM)” (see “References”), but applied to PMSM motor particularities.

The estimator has PLL structure. Its operating principle is based on the fact that the d-component of the Back Electromotive Force (BEMF) must be equal to zero at a steady state functioning mode. The block diagram of the estimator is presented in Figure 6.

Starting from the closed loop shown in Figure 6, the estimated speed (ω_{Restim}) of the rotor is integrated in order to obtain the estimated angle, as shown in Equation 1:

EQUATION 1:

$$\rho_{estim} = \int \omega_{Restim} dt$$

The estimated speed, ω_{Restim} , is obtained by dividing the q-component of the BEMF value with the voltage constant, K_Φ , as shown in Equation 2.

EQUATION 2:

$$\omega_{Restim} = \frac{1}{K_\Phi} (E_{qf} - \text{sgn}(E_{qf}) \cdot E_{df})$$

Considering the initial estimation premise (the d-axis value of BEMF is zero at steady state) shown in Equation 2, the BEMF q-axis value, E_{qf} , is corrected using the d-axis BEMF value, E_{df} , depending on its

sign. The BEMF d-q component's values are filtered with a first order filter, after their calculation with the Park transform, as indicated in Equation 3.

EQUATION 3:

$$E_d = E_\alpha \cos(\rho_{estim}) + E_\beta \sin(\rho_{estim})$$

$$E_q = E_\alpha \sin(\rho_{estim}) + E_\beta \cos(\rho_{estim})$$

With the fixed stator frame, Equation 4 represents the stators circuit equations.

EQUATION 4:

$$E_\alpha = V_\alpha - R_S I_\alpha - L_S \frac{dI_\alpha}{dt}$$

$$E_\beta = V_\beta - R_S I_\beta - L_S \frac{dI_\beta}{dt}$$

In Equation 4, the terms containing $\alpha - \beta$ were obtained from the three-phase system's corresponding measurements through Clarke transform. L_S and R_S represent the per phase stator inductance and resistance, respectively, considering Y (star) connected stator phases. If the motor is Δ (delta) connected, the equivalent Y connection phase resistance and inductance should be calculated and used in the equations above.

Figure 7 denotes the estimator's reference electrical circuit model. The A, B and C terminals of the motor are connected to the inverter's output terminals. The voltages, V_A , V_B and V_C , represent the phase voltages applied to the motor's stator windings. V_{AB} , V_{BC} and V_{CA} , represent the line voltages between the inverter's legs, while the phase currents are I_A , I_B and I_C .

FIGURE 6: PLL ESTIMATOR'S BLOCK SCHEMATIC

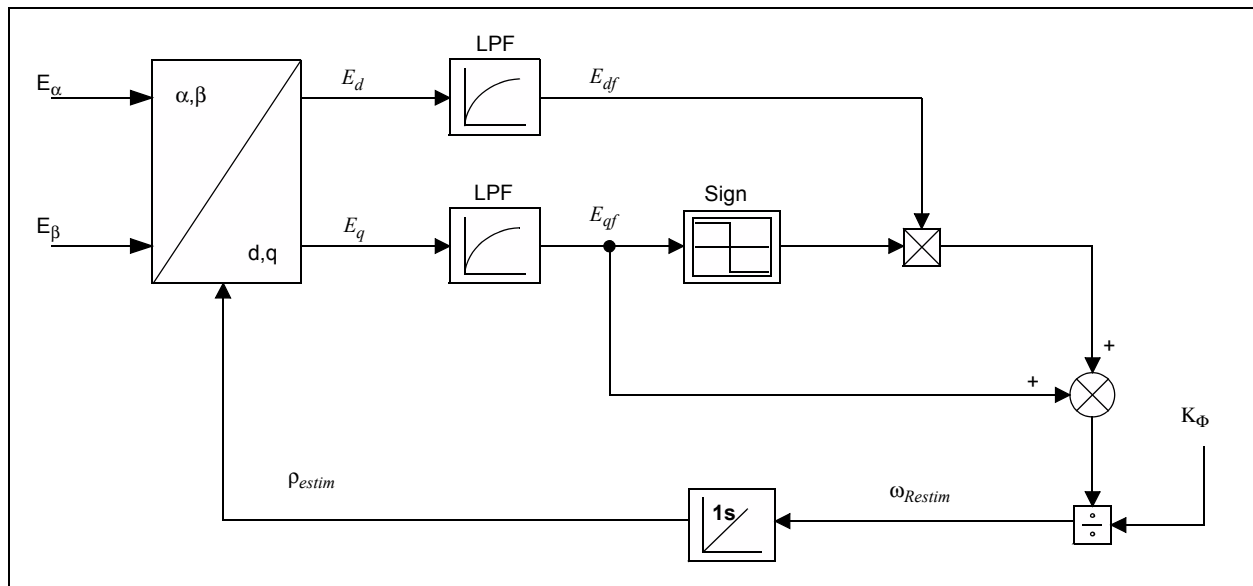
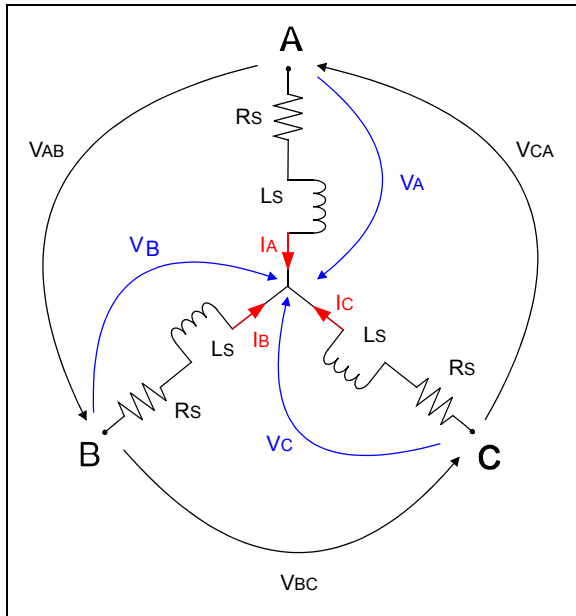


FIGURE 7: ELECTRICAL CIRCUIT MODEL FOR PLL ESTIMATOR



Taking one step forward concerning the equations implementation in the control system, the voltages V_α and V_β , implied in estimator's Equation 4 are a previous cycle calculation of the FOC, being fed to the Space Vector Modulation (SVM) block on the previous step of control, but also to the estimator block current step. I_α and I_β are Clarke transform results from the phase currents, which are read every estimator cycle.

The stator's inductance (L_S) and resistance (R_S) in Equation 4, are normalized and adapted to ease the computation and to satisfy the software representation requirements, as shown in Equation 5.

EQUATION 5:

MotorEstimParm.qLsDt representing:

$$\frac{L_S_NORM}{dt} = \frac{1}{T_S} \frac{U_0}{L_S I_0} \omega_0 \cdot 2^{15}$$

Where:

L_S = Motor phase inductance for Y connection

T_S = Sampling time equal to PWM period

$U_0 = \frac{U_N}{2^{15}}$, with U_N being the DC link voltage of the inverter

$I_0 = \frac{I_{peak}}{2^{15}}$, with I_{peak} being the maximum peak current per phase

$$\omega_0 = \frac{2 \cdot \pi}{60}$$

and,

MotorEstimParm.qRs representing:

$$R_S_NORM = R_S \frac{U_0}{I_0} \cdot 2^{15}$$

Where:

R_S = Motor phase resistance for Y connection

In the last term of Equation 4, the derivative of current to time is noisy in software; therefore, a limiting value for the current variation per estimator execution loop was introduced, which must be less than the maximum current variation per one estimator execution loop, which is done every PWM interrupt.

The resulting E_α and E_β values of BEMF are translated to the rotating reference frame of the rotor flux through the Park transform resulting in E_d and E_q values, which conform to Equation 3. The angle ρ_{estim} , used in Park transformation is calculated on the previous execution cycle of the estimator. The d-q values of BEMF are then filtered using first order filters, entering the main condition of the estimator, based on E_d being equal to '0'.

Equation 2 reflects the calculation of ω_{Restim} , which is the resulting electrical speed. The integrated electrical speed provides the angle (ρ_{estim}) between the rotor flux and the $\alpha - \beta$ fixed stator frame. In Equation 2, K_Φ denotes the voltage constant as indicated in Table 1. The normalized K_Φ used in the electrical speed computation, is shown in Equation 6.

EQUATION 6:

MotorEstimParm.qInvKFi represents:

$$\frac{1}{K_\Phi_NORM} = \frac{U_0}{\omega_0} \sqrt{3} \cdot 2 \cdot \pi \frac{1000}{60} \cdot P \cdot 2^{15}$$

Where:

P = Number of pole pairs and the other inputs indicated previously

The speed feedback is filtered using a first order filter identical with the one used in the BEMF case. The filter's generic form is shown in Equation 7:

EQUATION 7:

$$y(n) = y(n - 1) + K_{filter} \cdot (x(n) - y(n - 1))$$

Where:

$y(n)$ = Current cycle filter output

$y(n - 1)$ = Previous cycle filter output

$x(n)$ = Current cycle filter input

K_{filter} = Filter constant

The DC type values at the filter's output should be free of noise from the ADC acquisition or high-frequency variations introduced by the software calculations. The filter's tuning depends on how fast the filtered values (BEMF d-q components and electrical speed) can vary, allowing for sufficient bandwidth, which reduces the possibility of useful signal loss. In the case of BEMF d-q components, two situations can be identified: (1) high speed, in the Field Weakening mode, where their variation is slow due to the lack of sudden torque change or high acceleration ramp, and (2) low speed. The speed variation depends on the mechanical constant of the motor (and the load coupled on the motor's shaft) and the slope of the ramp-up or ramp-down limits on the speed reference, whichever is faster.

FIELD WEAKENING (FW)

The field weakening for PMSM implies imposing a negative value for the stator current on the rotating frame's d-axis, which has the role of weakening the air gap flux linkage.

The voltage output by the inverter, drops on the stator's resistance and inductive reactance, the remainder being used to counteract BEMF. BEMF is proportional with the motor's speed and the voltage constant, K_{Φ} , of the motor. Considering the limitation of the inverter's maximum output voltage, an increase in speed can be achieved by decreasing the motor's voltage constant K_{Φ} , which is proportional with the air gap flux linkage. Of course, a decrease in air gap flux linkage is synonymous to a torque decrease.

Things get a bit complicated at this point due to the complex relationship between the motors' characteristic parameters implied in the control of the air gap field weakening.

The effect of the armature d-axis current over the air gap field weakening depends on the shape and magnetic properties of the magnetic circuit starting from the armature teeth to the rotor's core. As stated previously, the type of surface mounted PM do not benefit effective field weakening; therefore, it is possible that the motor's magnetic circuit should be

designed only for base speed functioning and consequently, the saturation phenomena to occur whenever the base speed is exceeded. The saturation effect is responsible for electrical parameters variation – it is the case for the stator's linkage inductivity, which decreases in the Field Weakening mode.

The determination of such characteristics is a time-consuming process, the characteristics being, as expected, highly non-linear.

TUNING AND EXPERIMENTAL RESULTS

The algorithm tuning is very straight forward for speeds below the base speed, where the maximum torque mode is applied. Basically, the motor's parameters, measured or indicated by the manufacturer, are added to the support file, `tuning_params.xls`, which is provided with this application note (see **Appendix A: "Source Code"**), resulting in the normalized parameters for the estimator use. The values are then added to the `userparams.h` project file and are ready to run.

The measurement of parameters comprises the rotor's resistance, R_S , and inductance, L_S , and the voltage constant, K_{Φ} .

The stator resistance and induction can be measured at the motor's terminals, the reading value being divided by 2 to get the L_S and R_S values. For delta connected motors, if the manufacturer provides the phase resistance and inductance, their values should be divided by 3 to obtain the star connected motor equivalent phase resistance and inductance – R_S and L_S .

This voltage constant, K_{Φ} , is indicated by all motor manufacturers; however, it can be measured using a very simple procedure as well, by rotating the rotor shaft with a constant speed, while measuring the output voltage at the motor's terminals. If the reading is done at 1000 RPM, the alternative voltage measure is a typical RMS value. Multiplying the reading value by the square root of 2 will return the value in V_{peak}/K_{RPM} .

For the tested motor parameters, the data in Table 1 was measured with the procedures described above.

TABLE 1:

Motor Type	Hurst Motor DMB00224C10002	Units
Connection type	Y	—
L-L Resistance	1.92 · 2	Ohms
L-L Inductance – 1 kHz	2.67 · 2	mH
Voltage constant K_{Φ}	7.24	V_{peak}/K_{RPM}
Ambient temperature	22.7	°C

AN1292

The two necessary phase currents are read on the two shunts available on the dsPICDEM MCLV Development Board, and after ADC acquisition, their value being scaled to the convenient range. The overall current scaling factor depends on the gain of the differential Op amp reading the shunt and the maximum value of the current passing through the motor. For example, having a phase current of 4.4A peak and a gain of 75, for a 0.005 Ohms shunt resistor, results in 3.3V present at the ADC input. Considering a scaling factor of 1 for the current, translated in Example 1, the resulting currents will be in Q15 format, adapted to the software implementation necessities.

EXAMPLE 1:

```
#define KCURRA Q15(-0.5)
#define KCURRB Q15(-0.5)
```

In the support file, `tuning_params.xls`, the current scaling factor was determined experimentally, rather than by using the procedure above, thereby eliminating possible calculation errors due to electrical components tolerances. The scaling constant, shown in Equation 8, represents the value by which multiplying the internal software variable results in the real current value.

EQUATION 8:

$$I_0 = \frac{I_{peak}}{2^{15}}$$

Conversely, to obtain the scaling constant, the division of real current to the decimal number representing it in software is necessary in practice. This is accomplished using a current probe and MPLAB® IDE's Data Monitor and Capture Interface (DMCI) capability, measuring the peak current on the scope and dividing the value by the DMCI indicated counterpart, at a steady state of functioning. Please consult the MPLAB IDE help file for details on DMCI usage.

Equation 4 indicates that the acquisition current is implied in the resistive and inductive reactance voltage drop calculation. Due to the fact that the acquisition may be noisy, the derivative term implied in the inductive reactance voltage drop needs to be limited so that valid results will be obtained. For the motor tested, at a maximum speed of 5500 PRM and peak-to-peak current of 5A, the maximum current variation would be of 0.25A per 50 μs.

With respect to the initial calibration, the startup may be done with load, in which case the open loop ramp parameters need to be tuned.

The open loop tuning parameters include the lock time, the end acceleration speed, and the current reference value. The lock time represents the time necessary for rotor alignment, which depends on the load initial torque and moment of inertia (the larger they are, the larger the lock time value). The end speed of the initial ramp in RPM should be set sufficiently high for the estimator's calculated BEMF to have enough precision, while the time to reach that speed depends on the resistant load attached on the motor's shaft; the larger the load, the longer the time needed for reaching the end reference speed.

The open loop is implemented as a simplification of the closed loop control, where the estimated angle between the rotor flux and the fixed reference frame is replaced by the forced angle used in open loop speed-up. The forced angle does not care about the rotor's position, but rather imposing its position, being calculated as a continuous increment fraction. An additional simplification from the control loop presented in Figure 1, is the lack of the speed controller and the current reference for the q-axis being hard-coded.

The q-axis current reference is responsible for the current forced through the motor in the open loop ramp-up; the higher the initial load, the higher the current needed, which acts as a torque reference overall.

The macro definition for current references setup, as shown in Example 2, normalizes the real current value input parameter to the software required range, with its computation depending on the current scaling constant, initially determined through calculations (`NORM_CURRENT_CONST`). The real current value accepted as input should be in Amps and within the margins of $[-I_{peak}, I_{peak}]$.

EXAMPLE 2:

```
#define NORM_CURRENT(current_real)
(Q15(current_real/NORM_CURRENT_CONST/32768))
```

To keep the algorithm functioning in open loop, thus disabling the closed loop transition for initial tuning purposes, enable the specific code macro definition, as shown in Example 3.

EXAMPLE 3:

```
#define OPEN_LOOP_FUNCTIONING
```

This is particularly useful for the potential PI controller's recalibration or even some initial transition conditions verifications (such as angle error between the imposed angle and the estimated one, current scaling constant experimental determination), and initial open loop ramp up parameters fine tuning, previous to the closed loop activation.

For the speeds above the nominal speed, where field weakening is implied, the tuning is more sophisticated as the system parameter's non-linearity is involved.

The purpose of tuning starting from this point is to achieve a nominal speed doubling for the tested motor, in no load conditions.

Caution: Usually, the motor manufacturer indicates the maximum speed achievable by the motor without it being damaged (which could be higher than the brake point speed at rated current), but if not, it is possible to run it at higher speeds but only for small functioning periods (intermittent) assuming the risks of demagnetization or mechanical damage enunciated in the previous section.

In Field Weakening mode, if the FOC is lost at high speed above the nominal value, the possibility of damaging the inverter is imminent. The reason is that the BEMF will have a greater value than the one that would be obtained for the nominal speed, thereby exceeding the DC bus voltage value, which the inverter's power semiconductors and DC link capacitors would have to support. Since the tuning proposed implies iterative coefficient corrections until the optimum functioning is achieved, the protection of the inverter with corresponding circuitry should be assured in case of stalling at high speeds.

The Tuning principle explanation starts from the vector diagram in Figure 4. Considering the current required for maximum torque per amp generation at the maximum voltage that can be provided by the inverter, below nominal speed it represents only the q component, which is necessary for torque generation. For now, I_q equals I_S ; however, starting the field weakening strategy, the stator current I_S will be equal to the vectorial summation of the d and q components. Assuming a constant stator current I_S and input voltage U_S (in absolute value), the voltage drop on the stator resistance will be constant, while the inductive reactance drop will increase proportional with the speed. However, since the inductance value is very low for a surface mounted PM, the inductive reactance rise can be neglected when comparing to the other implied indicated measures. Taking into account this premise, when accelerating the motor, in field weakening the BEMF can be considered constant, a small decrease being accepted due to the increase of inductive reactance voltage drop.

With these in mind and considering Equation 6, a proportional relationship exists between the speed ω_R and $1/K_\Phi$, when keeping the BEMF constant, as shown in Equation 9.

EQUATION 9:

$$BEMF = \omega_R K_\Phi$$

Therefore, for speed doubling, consider an increase of more than half (125%) of one per voltage constant $1/K_\Phi$, to cover the inductive reactance voltage drop. The variation of $1/K_{\Phi_NORM}$ with the speed will be filled in a lookup table with the index depending on the speed. For the beginning, the table will represent the linear variation of $1/K_{\Phi_NORM}$ with the speed ω_R , but the linear variation can be finely tuned to obtain the best efficiency later on, depending on the load profile. The index in the lookup is obtained by subtracting the speed starting from which the field weakening strategy is applied from the actual speed of the rotor and dividing with a scaling factor. The indexing scaling factor gives a measure of the granularity of the lookup table, so that, for the same speed range, having a greater scaling factor results in fewer points in the lookup table, representing the considered speed domain. For the motor considered, the maximum speed is 27500 units, where 5000 units represent 1000 RPM. Considering a scaling factor equal to 1024, while the field weakening start speed is 13000 units, results in $(27500 - 13000) \div 1024 = 14.1$. Approximately 15 entries in the table are sufficient for covering the desired speed range. Reverse engineering, for 17 entries in the lookup table, the maximum speed possible would be $17 \cdot 1024 + 13000 = 30408$ units, approximately 6000 RPM. Due to the fact that the current estimated speed is somehow noisy and the index calculation can become unstable from one speed value to the other, in software, instead of the current speed (estimated), the reference speed is used for the index calculation. This is possible considering the reference speed variation ramp is sufficiently slow to allow the estimated speed to follow it closely.

Considering a linear variation between the base and the maximum speed, the lookup table values will look like Example 4 and the values will be updated with the experimental obtained results. The first value in this table represent the $1/K_\Phi$ value at the motor's base speed, as calculated using the support file (`tuning_parameters.xls`).

EXAMPLE 4: VOLTAGE CONSTANT INVERSE INITIALIZATION LOOKUP TABLE

```
#define INVKFI_SPEED0 7900
#define INVKFI_SPEED1 8600
#define INVKFI_SPEED2 9300
#define INVKFI_SPEED3 10000
#define INVKFI_SPEED4 10700
#define INVKFI_SPEED5 11400
#define INVKFI_SPEED6 12100
#define INVKFI_SPEED7 12800
#define INVKFI_SPEED8 13500
#define INVKFI_SPEED9 14200
#define INVKFI_SPEED10 14900
#define INVKFI_SPEED11 15600
#define INVKFI_SPEED12 16300
#define INVKFI_SPEED13 17000
#define INVKFI_SPEED14 17700
#define INVKFI_SPEED15 18500
#define INVKFI_SPEED16 19200
#define INVKFI_SPEED17 19750
```

Running the motor at nominal current will not result in permanent demagnetization of the magnets. Therefore, imposing nominal current to the d-component responsible with the air gap's net flux density decrease will not have a destructive effect. The q-component required for no load operation will be very small at steady state due to slow acceleration ramp and no resistant torque (except frictions in the bearings and fan). In practice, the d-axis current component is set via a lookup table with the same indexing used for the voltage constants lookup. Initially, the table will be filled with a linear variation of current I_d with speed ω_R (the first entry in the table represents the base speed value of I_{dref} and the last represents the nominal current value), as shown in Example 5.

EXAMPLE 5: REFERENCE D-AXIS CURRENT INITIALIZATION LOOKUP TABLE

```
#define IDREF_SPEED0 NORM_CURRENT(0)
#define IDREF_SPEED1 NORM_CURRENT(-0.09)
#define IDREF_SPEED2 NORM_CURRENT(-0.18)
#define IDREF_SPEED3 NORM_CURRENT(-0.27)
#define IDREF_SPEED4 NORM_CURRENT(-0.36)
#define IDREF_SPEED5 NORM_CURRENT(-0.45)
#define IDREF_SPEED6 NORM_CURRENT(-0.54)
#define IDREF_SPEED7 NORM_CURRENT(-0.63)
#define IDREF_SPEED8 NORM_CURRENT(-0.72)
#define IDREF_SPEED9 NORM_CURRENT(-0.81)
#define IDREF_SPEED10 NORM_CURRENT(-0.9)
#define IDREF_SPEED11 NORM_CURRENT(-0.99)
#define IDREF_SPEED12 NORM_CURRENT(-1.08)
#define IDREF_SPEED13 NORM_CURRENT(-1.17)
#define IDREF_SPEED14 NORM_CURRENT(-1.26)
#define IDREF_SPEED15 NORM_CURRENT(-1.35)
#define IDREF_SPEED16 NORM_CURRENT(-1.44)
#define IDREF_SPEED17 NORM_CURRENT(-1.53)
```

The negative d-component of the current will have the effect of decreasing the voltage constant K_ϕ , proportionally in the ideal case, leaving more space for speed increase as previously described.

Another aspect is the variation of the stator's linkage inductance in the Field Weakening mode, which is also non-linear. To counteract this effect, another lookup is implied with the same indexing as previously indicated. The value in the lookup represents the inductance $LS_{NORM}(\omega)/dt$ at the speed ω denoted by its index divided by the double of LS_{NORM}/dt at the base speed ω_0 . The first value in the table should always be one-half since the base speed inductance is divided by its own doubled value. At this point, the rest of the table will be filled in with values as if the inductance is half that of the base speed (Example 6).

EXAMPLE 6: INDUCTANCE VARIATION INIT LOOKUP TABLE

```
#define LS_OVER2LS0_SPEED0 Q15(0.5);
#define LS_OVER2LS0_SPEED1 Q15(0.25);
#define LS_OVER2LS0_SPEED2 Q15(0.25);
#define LS_OVER2LS0_SPEED3 Q15(0.25);
#define LS_OVER2LS0_SPEED4 Q15(0.25);
#define LS_OVER2LS0_SPEED5 Q15(0.25);
#define LS_OVER2LS0_SPEED6 Q15(0.25);
#define LS_OVER2LS0_SPEED7 Q15(0.25);
#define LS_OVER2LS0_SPEED8 Q15(0.25);
#define LS_OVER2LS0_SPEED9 Q15(0.25);
#define LS_OVER2LS0_SPEED10 Q15(0.25);
#define LS_OVER2LS0_SPEED11 Q15(0.25);
#define LS_OVER2LS0_SPEED12 Q15(0.25);
#define LS_OVER2LS0_SPEED13 Q15(0.25);
#define LS_OVER2LS0_SPEED14 Q15(0.25);
#define LS_OVER2LS0_SPEED15 Q15(0.25);
#define LS_OVER2LS0_SPEED16 Q15(0.25);
#define LS_OVER2LS0_SPEED17 Q15(0.25);
```

For testing purpose, a slow software ramp is implemented as a speed reference, being activated using the following definition, as shown in Example 7.

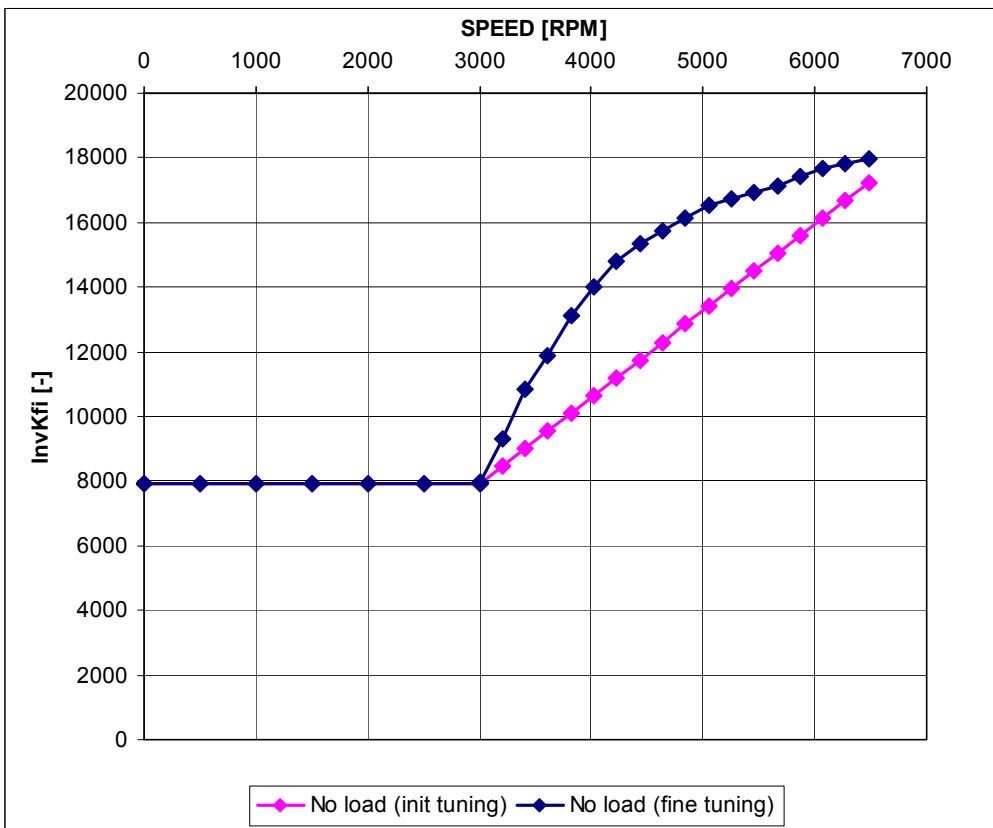
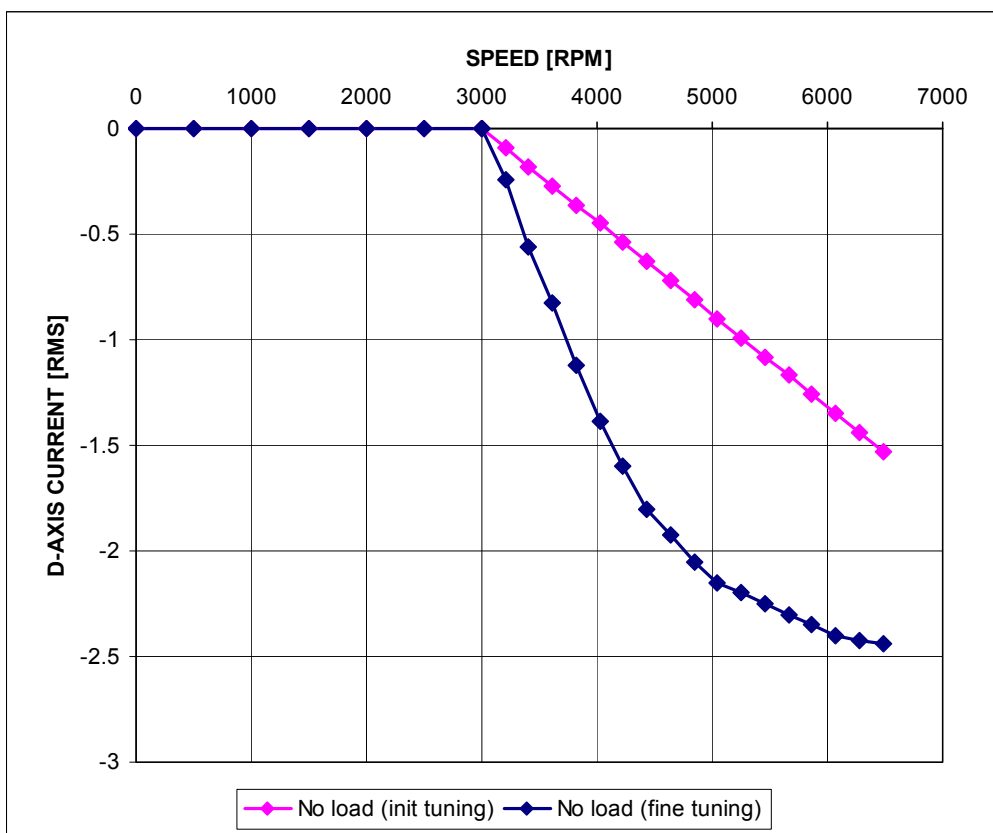
EXAMPLE 7:

```
#define TUNING
```

If the results of running the software in these conditions will stall the motor at a speed higher than nominal, it is due to the fact that the lookup tables were filled with estimative values, which at some point do not match the real non-linearities. Immediately, once the motor stalls, halt the program execution, capturing the value of the index (`FdWeakParm.qIndex`) in the debugger watch window. The index indicates the point where the values of I_{dref} in ascending order, were not effective and should be updated. In order to further improve the performance, the value indicated by the current index in the lookup table should be replaced by the value indicated by the next index (`FdWeakParm.qIndex + 1`) and the motor's behavior should be checked again. The achievable speed should increase and repeating this process for several times the maximum speed for the nominal current reference imposed on d-axis will be reached. If the maximum speed obtained for the nominal current is not the targeted one (meaning double the nominal speed in this case) the absolute value of the d-axis current reference should be increased above the nominal value. The d-current reference increase should be started from the value denoted by the index where the motor stalled. The index value should correspond to the actual speed of the motor, measured at the shaft using a tachometer, keeping in mind that the lookup index is calculated using the reference speed not the actual estimated speed. In the case of the motor tested, it was possible to impose a d-axis current of one and a half times the nominal current, which almost doubles the base speed. The results of these operations leads to the data presented in Figure 8. Once the d-current increase will not have an effect in increasing the speed (increasing the current too much will generally stall the motor), the index corresponding to the stall will indicate where the value for inductance should be operated (increasing or decreasing its value). The inductance variation lookup table is the last to be updated.

For loaded tests, the initial condition, mainly the current on d-axis reference, which in field weakening equals the nominal current value, is no longer valid since the q-axis current is needed for torque generation. The ratio between the power to be used for field weakening and for torque generation depends on the load torque-speed characteristic.

FIGURE 8: D-AXIS CURRENT, $1/K_{\Phi}$ FUNCTION OF SPEED



Another concern during the Field Weakening mode is voltage limitation of the inverter. This voltage limitation is translated to the maximum achievable values for d-q current components. If both components would have followed their reference values, their resulting scalar summation value would overlap the maximum value of '1'. Therefore, the maximum current permitted for q-component of the current (the torque component of the current) will result from prioritizing the d-component of the current responsible field weakening, which is more important due to air gap field weakening purposes. Figure 9 presents this dynamic adjustment translated to the d-q component of the voltages (d-component of voltage prioritizing).

Due to the fact that estimator performance depends drastically on the parameters of the motor, the experimental results keep this premise for the conditions of the measurements. The first dependence of rotor resistance and flux constant of the motor is the temperature. A high torque is obtained using the maximum current input, resulting in high Joule losses, resulting in an increased motor temperature. This has a negative effect on the validity of the estimator's output. Please note that it is not the intention of this application note to correct or compensate for the effect of temperature on the estimation. The compensation of parameters with temperature is possible, but it varies considerably from one motor type to another, the

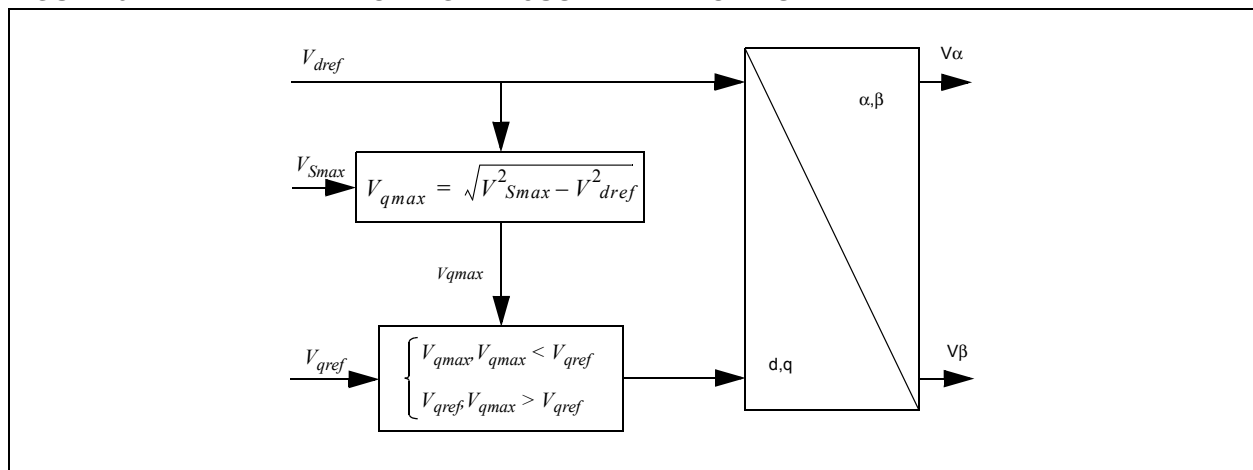
working conditions and functional mode. As a consequence, the test results indicated below have a premise that limits the temperature effect on the estimator's output – the time for the achieved torque is limited to one minute of continuous functioning at room temperature (see Table 2).

TABLE 2: EXPERIMENTAL RESULTS TESTS WITH LOAD

Reference Speed (RPM)	Achieved Speed (RPM)	Torque (Nm)	Phase Current (A RMS)
500	500	0.148	1.697
1000	1000	0.111	1.556
1500	1425	0.083	1.513
2000	1900	0.062	1.117
2500	2375	0.031	0.608
3000	2850	0.020	0.636
3500	3325	0.019	1.174
4000	3800	0.015	1.556

It may be observed that the phase current measured for the last two entries in Table 2, corresponding to the field weakening operation, are higher than the ones immediately preceding them, in normal operation speed.

FIGURE 9: DYNAMIC VOLTAGE ADJUSTMENT BLOCK SCHEMATIC



AN1292

The sensorless FOC algorithm uses the following resources in the software developed for a dsPIC33FJ32MC204, using the compiler's -O3 level optimization, in Release mode:

- Program memory (Flash): 5682 bytes (total)
 - 612 bytes (field weakening code)
 - 645 bytes (main user interface code)
 - 4425 bytes (sensorless FOC without field weakening code)
- Data memory (RAM):
 - 444 bytes (total without debug data dump arrays)

The time necessary measurement for the algorithm execution, running at 40 MHz core clock, using -O3 level compiler optimization have the following results:

- ADC Interrupt comprising the sensorless FOC algorithm with field weakening code execution:
 - Minimum: 14.975 μ s
 - Average: 23.325 μ s
 - Maximum: 23.65 μ s
- ADC Interrupt comprising the sensorless FOC algorithm without field weakening code execution:
 - Minimum: 14.725 μ s
 - Average: 20.8 μ s
 - Maximum: 21.4 μ s

The ADC Interrupt is executed every 50 μ s, being triggered every PWM period (PWM frequency is 20 kHz).

CONCLUSION

This application note describes a method of flux angle and speed estimation for Permanent Magnet Synchronous Motors (PMSM). This method is applied with success in the Field Weakening mode of PMSM, which greatly increases the types of possible applications.

The main theoretical ideas behind the estimator and most importantly, the tuning directions, are also discussed. The application described in this document uses support files for the ease of adapting it to other motors. Additionally, using the indicated development hardware platform offered by Microchip for your application can significantly shorten time-to-market.

REFERENCES

The following application notes, which are referenced in this document, are available for download from the Microchip Web site (www.microchip.com):

- AN908 *"Using the dsPIC30F for Vector Control of an ACIM"*
- AN1078 *"Sensorless Field Oriented Control of PMSM Motors using dsPIC30F or dsPIC33F Digital Signal Controllers"*
- AN1162 *"Sensorless Field Oriented Control (FOC) of an AC Induction Motor (ACIM)"*

APPENDIX A: SOURCE CODE

Software License Agreement

The software supplied herewith by Microchip Technology Incorporated (the "Company") is intended and supplied to you, the Company's customer, for use solely and exclusively with products manufactured by the Company.

The software is owned by the Company and/or its supplier, and is protected under applicable copyright laws. All rights are reserved. Any use in violation of the foregoing restrictions may subject the user to criminal sanctions under applicable laws, as well as to civil liability for the breach of the terms and conditions of this license.

THIS SOFTWARE IS PROVIDED IN AN "AS IS" CONDITION. NO WARRANTIES, WHETHER EXPRESS, IMPLIED OR STATUTORY, INCLUDING, BUT NOT LIMITED TO, IMPLIED WARRANTIES OF MERCHANTABILITY AND FITNESS FOR A PARTICULAR PURPOSE APPLY TO THIS SOFTWARE. THE COMPANY SHALL NOT, IN ANY CIRCUMSTANCES, BE LIABLE FOR SPECIAL, INCIDENTAL OR CONSEQUENTIAL DAMAGES, FOR ANY REASON WHATSOEVER.

All of the software covered in this application note is available as a single WinZip archive file. This archive can be downloaded from the Microchip corporate Web site at:

www.microchip.com

APPENDIX B: REVISION HISTORY

Revision A (September 2009)

This is the initial released version of this document.

AN1292

NOTES:

Note the following details of the code protection feature on Microchip devices:

- Microchip products meet the specification contained in their particular Microchip Data Sheet.
- Microchip believes that its family of products is one of the most secure families of its kind on the market today, when used in the intended manner and under normal conditions.
- There are dishonest and possibly illegal methods used to breach the code protection feature. All of these methods, to our knowledge, require using the Microchip products in a manner outside the operating specifications contained in Microchip's Data Sheets. Most likely, the person doing so is engaged in theft of intellectual property.
- Microchip is willing to work with the customer who is concerned about the integrity of their code.
- Neither Microchip nor any other semiconductor manufacturer can guarantee the security of their code. Code protection does not mean that we are guaranteeing the product as “unbreakable.”

Code protection is constantly evolving. We at Microchip are committed to continuously improving the code protection features of our products. Attempts to break Microchip's code protection feature may be a violation of the Digital Millennium Copyright Act. If such acts allow unauthorized access to your software or other copyrighted work, you may have a right to sue for relief under that Act.

Information contained in this publication regarding device applications and the like is provided only for your convenience and may be superseded by updates. It is your responsibility to ensure that your application meets with your specifications. MICROCHIP MAKES NO REPRESENTATIONS OR WARRANTIES OF ANY KIND WHETHER EXPRESS OR IMPLIED, WRITTEN OR ORAL, STATUTORY OR OTHERWISE, RELATED TO THE INFORMATION, INCLUDING BUT NOT LIMITED TO ITS CONDITION, QUALITY, PERFORMANCE, MERCHANTABILITY OR FITNESS FOR PURPOSE. Microchip disclaims all liability arising from this information and its use. Use of Microchip devices in life support and/or safety applications is entirely at the buyer's risk, and the buyer agrees to defend, indemnify and hold harmless Microchip from any and all damages, claims, suits, or expenses resulting from such use. No licenses are conveyed, implicitly or otherwise, under any Microchip intellectual property rights.

Trademarks

The Microchip name and logo, the Microchip logo, dsPIC, KEELOQ, KEELOQ logo, MPLAB, PIC, PICmicro, PICSTART, rPIC and UNI/O are registered trademarks of Microchip Technology Incorporated in the U.S.A. and other countries.

FilterLab, Hampshire, HI-TECH C, Linear Active Thermistor, MXDEV, MXLAB, SEEVAL and The Embedded Control Solutions Company are registered trademarks of Microchip Technology Incorporated in the U.S.A.

Analog-for-the-Digital Age, Application Maestro, CodeGuard, dsPICDEM, dsPICDEM.net, dsPICworks, dsSPEAK, ECAN, ECONOMONITOR, FanSense, HI-TIDE, In-Circuit Serial Programming, ICSP, Mindi, MiWi, MPASM, MPLAB Certified logo, MPLIB, MPLINK, mTouch, Octopus, Omniscient Code Generation, PICC, PICC-18, PICDEM, PICDEM.net, PICkit, PICtail, PIC³² logo, REAL ICE, rLAB, Select Mode, Total Endurance, TSHARC, UniWinDriver, WiperLock and ZENA are trademarks of Microchip Technology Incorporated in the U.S.A. and other countries.

SQTP is a service mark of Microchip Technology Incorporated in the U.S.A.

All other trademarks mentioned herein are property of their respective companies.

© 2009, Microchip Technology Incorporated, Printed in the U.S.A., All Rights Reserved.

 Printed on recycled paper.

**QUALITY MANAGEMENT SYSTEM
CERTIFIED BY DNV
== ISO/TS 16949:2002 ==**

Microchip received ISO/TS-16949:2002 certification for its worldwide headquarters, design and wafer fabrication facilities in Chandler and Tempe, Arizona; Gresham, Oregon and design centers in California and India. The Company's quality system processes and procedures are for its PIC® MCUs and dsPIC® DSCs, KEELOQ® code hopping devices, Serial EEPROMs, microperipherals, nonvolatile memory and analog products. In addition, Microchip's quality system for the design and manufacture of development systems is ISO 9001:2000 certified.



Worldwide Sales and Service

AMERICAS

Corporate Office

2355 West Chandler Blvd.
Chandler, AZ 85224-6199
Tel: 480-792-7200
Fax: 480-792-7277
Technical Support:
<http://support.microchip.com>
Web Address:
www.microchip.com

Atlanta

Duluth, GA
Tel: 678-957-9614
Fax: 678-957-1455

Boston

Westborough, MA
Tel: 774-760-0087
Fax: 774-760-0088

Chicago

Itasca, IL
Tel: 630-285-0071
Fax: 630-285-0075

Cleveland

Independence, OH
Tel: 216-447-0464
Fax: 216-447-0643

Dallas

Addison, TX
Tel: 972-818-7423
Fax: 972-818-2924

Detroit

Farmington Hills, MI
Tel: 248-538-2250
Fax: 248-538-2260

Kokomo

Kokomo, IN
Tel: 765-864-8360
Fax: 765-864-8387

Los Angeles

Mission Viejo, CA
Tel: 949-462-9523
Fax: 949-462-9608

Santa Clara

Santa Clara, CA
Tel: 408-961-6444
Fax: 408-961-6445

Toronto

Mississauga, Ontario,
Canada
Tel: 905-673-0699
Fax: 905-673-6509

ASIA/PACIFIC

Asia Pacific Office

Suites 3707-14, 37th Floor
Tower 6, The Gateway
Harbour City, Kowloon
Hong Kong
Tel: 852-2401-1200
Fax: 852-2401-3431

Australia - Sydney

Tel: 61-2-9868-6733
Fax: 61-2-9868-6755

China - Beijing

Tel: 86-10-8528-2100
Fax: 86-10-8528-2104

China - Chengdu

Tel: 86-28-8665-5511
Fax: 86-28-8665-7889

China - Hong Kong SAR

Tel: 852-2401-1200
Fax: 852-2401-3431

China - Nanjing

Tel: 86-25-8473-2460
Fax: 86-25-8473-2470

China - Qingdao

Tel: 86-532-8502-7355
Fax: 86-532-8502-7205

China - Shanghai

Tel: 86-21-5407-5533
Fax: 86-21-5407-5066

China - Shenyang

Tel: 86-24-2334-2829
Fax: 86-24-2334-2393

China - Shenzhen

Tel: 86-755-8203-2660
Fax: 86-755-8203-1760

China - Wuhan

Tel: 86-27-5980-5300
Fax: 86-27-5980-5118

China - Xiamen

Tel: 86-592-2388138
Fax: 86-592-2388130

China - Xian

Tel: 86-29-8833-7252
Fax: 86-29-8833-7256

China - Zhuhai

Tel: 86-756-3210040
Fax: 86-756-3210049

ASIA/PACIFIC

India - Bangalore

Tel: 91-80-3090-4444
Fax: 91-80-3090-4080

India - New Delhi

Tel: 91-11-4160-8631
Fax: 91-11-4160-8632

India - Pune

Tel: 91-20-2566-1512
Fax: 91-20-2566-1513

Japan - Yokohama

Tel: 81-45-471- 6166
Fax: 81-45-471-6122

Korea - Daegu

Tel: 82-53-744-4301
Fax: 82-53-744-4302

Korea - Seoul

Tel: 82-2-554-7200
Fax: 82-2-558-5932 or
82-2-558-5934

Malaysia - Kuala Lumpur

Tel: 60-3-6201-9857
Fax: 60-3-6201-9859

Malaysia - Penang

Tel: 60-4-227-8870
Fax: 60-4-227-4068

Philippines - Manila

Tel: 63-2-634-9065
Fax: 63-2-634-9069

Singapore

Tel: 65-6334-8870
Fax: 65-6334-8850

Taiwan - Hsin Chu

Tel: 886-3-6578-300
Fax: 886-3-6578-370

Taiwan - Kaohsiung

Tel: 886-7-536-4818
Fax: 886-7-536-4803

Taiwan - Taipei

Tel: 886-2-2500-6610
Fax: 886-2-2508-0102

Thailand - Bangkok

Tel: 66-2-694-1351
Fax: 66-2-694-1350

EUROPE

Austria - Wels

Tel: 43-7242-2244-39
Fax: 43-7242-2244-393

Denmark - Copenhagen

Tel: 45-4450-2828
Fax: 45-4485-2829

France - Paris

Tel: 33-1-69-53-63-20
Fax: 33-1-69-30-90-79

Germany - Munich

Tel: 49-89-627-144-0
Fax: 49-89-627-144-44

Italy - Milan

Tel: 39-0331-742611
Fax: 39-0331-466781

Netherlands - Drunen

Tel: 31-416-690399
Fax: 31-416-690340

Spain - Madrid

Tel: 34-91-708-08-90
Fax: 34-91-708-08-91

UK - Wokingham

Tel: 44-118-921-5869
Fax: 44-118-921-5820

03/26/09